Tellus (1983), *35A*, 219–230

A heat-flux history length scale for the nocturnal boundary layer

By ROLAND B. STULL, *Department of Meteorology, University of Wisconsin, 1225 West Dayton Street, Madison, WI 53706, U.S.A.*

(Manuscript received April 6; in final form July 20, 1982)

ABSTRACT

A height scale, $H = \int Q_H \, dt/(\rho C_p \, \Delta\theta_s)$, based on the night-time heat-flux (Q_H) history is proposed here as being a relevant scale for the nocturnal boundary layer temperature structure. This scale, together with the surface temperature decrease since sunset, $\Delta\theta_s$, are shown to be sufficient to define a common similarity shape for the potential temperature profile. An equation for this shape based on Wangara field experiment data is $\Delta\theta/\Delta\theta_s = \exp(-0.77z/H)$. This curve is then tested against the Koorin boundary-layer data set, and is shown to provide a good fit to the data. Such a potential-temperature profile equation suggests that the top of the boundary layer is at about $5H$, and that 23% of the cooling within that depth is caused directly by radiation. The definition for H, above, is shown to be a simple means of expressing much of the same information as Nieuwstadt's rate equation.

1. Introduction

Turbulence and mean-variable profiles within the nocturnal boundary layer (NBL) have not lent themselves to a manifest description of the boundary layer depth. Consequently, there is a debate in the micrometeorological community regarding how to define that depth. Tied to this debate, and equally unresolved, are parameterizations for various length scales or heights based on subsets of NBL physics.

The goals of this paper are fivefold:

(1) To define an accumulation-type of nocturnal length scale, H, based on the time-history of the surface heat flux.
(2) To propose an exponential similarity shape for the nocturnal potential temperature profile as an alternative to Yamada's (1979) cubic equation.
(3) To show that a scale such as H offers the simplicity-of-use of a diagnostic-type of scale, while incorporating much of the physics of the adjustment-type relationship of Nieuwstadt (1980).
(4) To examine the relationship between H and bulk turbulence characteristics.
(5) To support the inferences by Andre and Mahrt (1982) and Garratt and Brost (1981) regarding the importance of direct radiational cooling of the boundary-layer air.

In section 2, height definitions are broken into two major categories. Based on arguments in section 3 concerning the relationship between turbulence, heat flux, and profiles of mean potential temperature, an integral length scale is proposed in section 4. This scale is used to define dimensionless temperatures and heights, forming the basis for a similarity shape for the potential temperature profile (section 5). The equation for this shape is found empirically, using Wangara data, and tested independently with Koorin data in section 6. Discussions on the meaning and use of such length scales are pursued in sections 7 and 8. Relationships between the length scale and an adjustment equation are examined in section 9.

Questions regarding the wind profile in the NBL are not addressed here. Hence, results presented here concerning the temperature structure must be viewed as a study of just one piece of the NBL puzzle.

2. Nocturnal boundary layer depth

Mahrt (1981) has compiled an extensive bibliography of references dealing with the NBL. At first glance, there appears to be almost as many definitions of depth of the NBL as there are investigators.

There is a very good reason for this predicament. Contrary to the day-time mixed-layer case, there is no well-defined top to the NBL. Turbulence is intermittent, weak, and decreases with height from the surface. Temperature lapse rates weaken as the nocturnal inversion blends smoothly into the (often) adiabatic lapse rate above. Wind speeds oscillate inertially, and gravity waves frequently superimpose their characteristic signatures on the flow.

As a result, investigators have enjoyed the freedom to define heights that best relate to their topic of interest. Examples include heights where: the lapse rate becomes adiabatic, the wind speed is maximum (assuming that there always is such a nocturnal jet), the stress is 10% of its surface value, the heat flux is negligibly small, and the average turbulence intensity is near zero. Each of these definitions is definable in terms of some measurable characteristic of the flow. In this sense, they are fundamental definitions that are determined by nature. Thus, one must expect some physical (and mathematical) relationship can be found interrelating these hights.

In juxtaposition to these fundamental definitions are some secondary length scales that have been proposed. Such diagnostic scales are usually constructed from reduced sets of equations that partially define the night-time boundary layer flow. Examples of these definitions include the Ekman layer depth, u_*/f, the Obukhov length, $L = -Tu_*^3/(gk\overline{w'\theta'})$, and the bulk Richardson number, $R_B = g\Delta\theta\Delta z/(\theta\Delta U^2)$, where u_* is the friction velocity, f is the Coriolis parameter, T is absolute temperature, g is the acceleration due to gravity, k is the von Karman constant, $\overline{w'\theta'}$ is the vertical kinematic component of turbulent heat flux, and where $\Delta\theta$ and ΔU represent potential temperature and mean wind speed changes across a vertical height increment of Δz. Theoretical and/or empirical relationships can then be pursued that can diagnose or predict the appropriate length scale. Adjustment or relaxation approaches have been a popular means of tying diagnostic scales to prediction equations.

One hopes that the predictable or diagnosable secondary length scales are in some way related to the fundamental definitions of boundary layer depth.

The purpose of this paper is to describe an additional secondary length scale based on the accumulated surface-induced cooling that occurs during the night. This scale, called a heat-flux history length scale, can be used in certain situations to diagnose one of the fundamental definitions of the NBL depth: namely the thickness of the layer of air that has been cooled because of the presence of the ground. For the Wangara and Koorin field experiments, this often is just the thickness of the statically-stable layer of air adjacent to the ground.

3. Instantaneous fluxes versus the time integral of flux

In the next few paragraphs, we will attempt to show that the stable boundary layer is, in part, controlled by the time-integrated value of surface heat flux. Under this hypothesis, the instantaneous heat flux value is, by itself, of less importance. The relationship between heat flux, turbulence, and mean vertical profiles forms the essence of the arguments below. Assume, for simplicity, a horizontally uniform environment where advection terms can be neglected, and where horizontal averaging over about a 100 km^2 area is implied for the various mean quantities.

Given that the earth's surface cools at a rate governed by radiative effects at night, one recognizes that there is a cooling imposed on the very lowest layers of air due to molecular conduction to this cold surface. Molecular processes alone can not account for the thick (hundreds of meters) nocturnal inversions that are frequently observed over land. It has long been recognized that turbulence is a mechanism contributing to the observed temperature distributions.

Turbulence in a stably-stratified boundary layer occurs due to wind shear effects. The local value of gradient Richardson number has been used with much success to diagnose the local occurrence of turbulence. Thus, the mean wind and temperature profiles are critical influences governing the nature of turbulence at night. As cooling of the air evolves, regions of locally reduced Richardson number may appear and disappear, favoring intermittent periods of turbulence with the corresponding turbulent diffusion of heat and momentum.

Contrast this with the day-time situation where insolation generates large positive values of heat flux at the surface. The surface layer and mixed layer are usually continuously turbulent, with the only intermittency occurring within the entrainment zone at the top of the mixed layer. Variations in surface heat flux cause rapid responses in turbulence intensity and vertical transport throughout much of the mixed layer due to the mechanism of plumes and thermals. The response time for communication of surface characteristics to the rest of the boundary layer is of the order of 10–20 min. The turbulence structure in the day-time boundary layer is thus nearly in equilibrium with the surface forcings.

At night, variations in surface heat flux are not communicated as rapidly to the rest of the boundary layer. As Brost and Wyngaard (1978) have suggested, the turbulence structure may not be able to reach equilibrium with the surface forcings because of response times of the order of 1–18 h. In spite of this, the effects of the surface heat flux are being accumulated within the NBL, as evidenced by the growing strength and thickness of the nocturnal inversion. This accumulation process modifies the average lapse rate within the NBL, and thus acts as one of the controls on turbulence as discussed above using Richardson number arguments.

The arguments above support the hypothesis that the instantaneous heat flux may not be a governing parameter of the flow. Turbulence, as well as the mean structure of the NBL, depends on the time-history of quantities such as the heat flux. This hypothesis is verified with two independent data sets in sections 5 and 6.

4. A heat flux history scale

Define the transition time as that instant when the net sensible heat flux into the air at the earth's surface changes sign from positive to negative. For the fair-weather evenings considered in this study, this transition often occurs 30 to 60 min prior to sunset. At this transition time, the lapse rates observed during both the Wangara and Koorin field programs are nearly adiabatic from the surface up to at least 1 km.

As the night progresses, the surface air temperature cools from its initial value at transition time. Denote the magnitude of the surface potential temperature change by $\Delta\theta_s = \theta_s(t) - \theta_0$, where θ_0 is the potential temperature of the adiabatic profile at transition time and $\theta_s(t)$ is the surface potential temperature found at time t since transition. See the Appendix for a more detailed description of θ_0. The surface values are based on air temperatures measured at standard instrument shelter height (about 1 m above ground), rather than on the cooler "skin" temperature of the ground itself. Note that $\Delta\theta_s$ defines a temperature scale.

Define a nocturnal integral operator, I, by

$$I(\phi) = \int_0^t \phi \, d\tau \qquad (1)$$

where ϕ represents any variable, and τ is a dummy of integration. Next, define a heat-flux-history length scale, H, by

$$H = I(Q_H/\rho C_p)/\Delta\theta_s \qquad (2)$$

where Q_H is the net vertical heat flux impressed onto the boundary layer at the earth's surface, ρ is the density of air, and C_p is the specific heat of air at constant pressure.

A positive value for heat flux corresponds to heating of the air. Hence, the negative values of Q_H and $\Delta\theta_s$ at night define a positive value for the length scale, H. As described in the Appendix, Q_H is defined by a surface radiation balance, and is not based on the existence or non-existence of a turbulence heat flux.

The form of (2) written above was selected without including any time-weighting factors within the integral operator. Thus, H reflects the total accumulated cooling that has occurred since transition, regardless of whether the bulk of the cooling occurred early or late in the night. Such an approach allows easy interpretation of H in terms of the layer-averaged heat-balance equation, as is discussed in section 7.

The temperature and length scales defined above form the basis for the potential temperature similarity profiles presented in the next section.

For the special case where the heat flux is achieved by predominantly turbulent motions, then

$Q_H = \rho C_p(\overline{w'\theta'})_s$. The length scale can then be rewritten in a simpler form, $H = I(\overline{w'\theta_s'})/\Delta\theta_s$, where the overbar indicates an average over a large horizontal area, say 100 km^2. $w'\theta_s'$ is the effective near-surface kinematic turbulent heat flux.

5. Similarity profiles of potential temperature

It is proposed that vertical profiles of nocturnal potential temperatures are similar to each other when the dimensionless potential temperature change, $\Delta\theta/\Delta\theta_s$, is plotted against the dimensionless height, z/H. This similarity should be observed over level terrain that is horizontally uniform, with an air mass that is also horizontally uniform throughout the depth of the boundary layer. The dimensional potential temperature change at any height is defined analogously to the surface value; namely, $\Delta\theta = \theta(t, z) - \theta_0$, where θ is the potential temperature measured at height z.

The similarity hypothesis proposed here is verified with Wangara field experiment data (Clarke et al., 1971). Periods are discarded from this data set that are under the influence of low pressure systems or fronts. Additional periods of probable instrument errors, and periods where rain or thunderstorms were in the vicinity are also discarded. The remaining data set consists of 40 observations over 12 nights, with observation times ranging from 18 to 6 local time (Eastern Australian Time = Greenwich Mean Time + 10 hours).

Yamada (1979) showed that a similar scaling was successful, when tested with soundings from five Wangara nights. His height was made nondimensional using the total thickness of the stable layer, h, rather than the integral length scale used here. As will be demonstrated in section 8, h is directly proportional to H.

Fig. 1 presents the nocturnal Wangara data plotted in dimensionless coordinates. A total of 654 data points are plotted. Table 1 lists the length and temperatures scales for each observation time. Heat flux for these calculations was found from a simplified surface energy budget equation (see the Appendix), using only net radiation and ground heat flux.

The degree of scatter of the data points is partially due to the assumptions given earlier in this section not being satisfied. In particular, even the gentle slopes at Hay, Australia may have been sufficient to generate weak drainage winds (Brost and Wyngaard, 1978). Also, the influences of buoyancy (gravity) waves and advection may have infiltrated the data.

The shape of the data in Fig. 1 suggests that an exponential curve would provide a good fit to the data.

$$\Delta\theta/\Delta\theta_s = \exp(-az/H) \tag{3}$$

Using the method of least squares, where dimensionless height was the independent variable, and where the exponential was forced to pass through a dimensionless temperature change of unity at the earth's surface, one finds that $a = 0.77$ gives the best fit. This regression explains 91% of the total variance for $0 < z/H < 9$. Over the interval of $0 \leq z/H \leq 5$, where the scatter is greatest, the regression explains only 88% of the total variance.

The shape of (3) is similar to the shape of Yamada's (1979) third-order polynomial (Fig. 5), and is offered as an alternative for Yamada's parameterization. Both are constructed to empirically fit the data, although Yamada's curve diverges away from the data above h, and therefore is limited to a domain of $0 < z < h$. Equation (3) has the advantages that it fits the observed potential temperature profiles to heights well above h, and that it does not explicitly use h, a quantity that is sometimes difficult to determine.

The exponential shape of (3) is significantly different from the shape found by Izumi and Barad (1963). For a very intense nocturnal jet (about 30 m s^{-1} at 300 m) over Texas, they found night-time temperature profiles characterized by a thick layer of mildly stable air near the ground, capped by a layer of increased stability. As the night progressed, the temperature profile evolved into a state that more resembled a turbulent mixed layer capped by a strong inversion. This shape profile is not evident in the Wangara data, even on those days of strongest nocturnal jet speed (of the order of 15 m s^{-1}). One explanation for this difference, other than the obvious one that the speed was slower, might be a difference in roughness between the two sites. Another possibility is that there is some critical value of the bulk nocturnal Richardson number, below which the flow tends towards a mixed layer rather than an exponentially-shaped potential temperature profile.

Wetzel (1982) has proposed a three-layer parameterization for the nocturnal temperature inver-

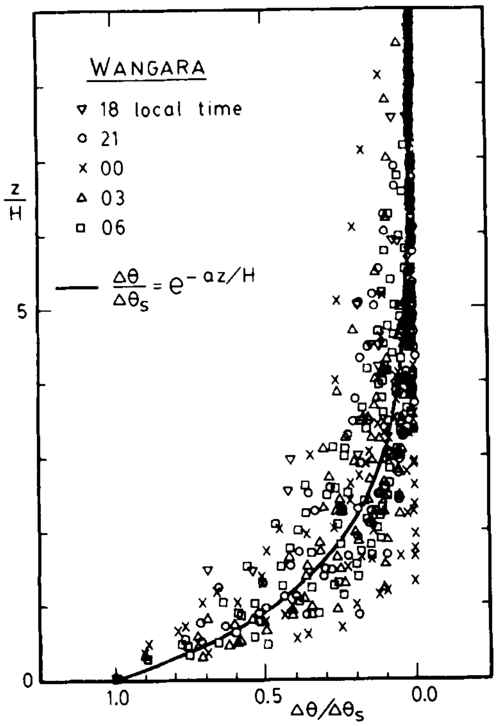

Fig. 1. Dimensionless potential temperature plotted against dimensionless height, using observations of the nocturnal temperature inversion made during the Wangara experiment. The solid curve represents the least-squares best fit of an exponential shape to the data, with $a = 0.77$.

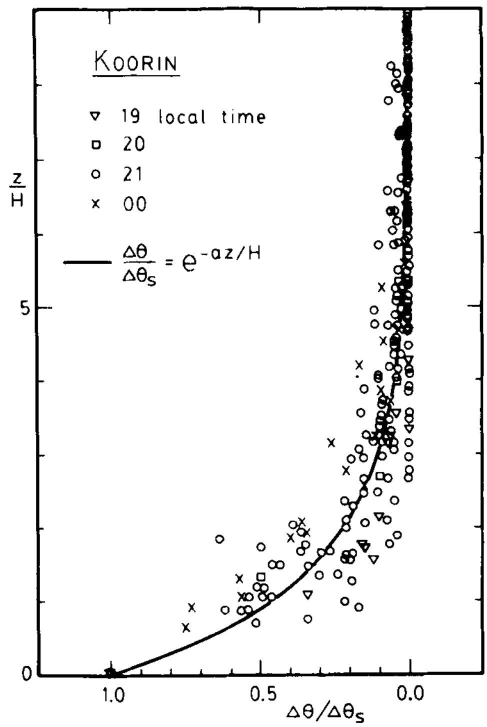

Fig. 2. Same as Fig. 1, but for the Koorin data set.

sion, where the middle of the inversion has a linear potential temperature profile. It appears that the exponential shape (3) and Wetzel's three-layer model both provide a good fit to the Wangara data.

6. An independent test

Data from the Koorin field experiment were used as an independent test of the similarity hypotheses (Clarke and Brook, 1979). This experiment was conducted near Daly Waters in northern Australia, where the tropical easterly winds provided an environment different from the westerlies of the extratropical Wangara experiment.

Transition usually occurred near 18 local mean time (GMT + 9.5 hours). Except for an occasional 19 or 20 local-time sounding, most of the nocturnal temperature data start with the 21 local time sounding. Unfortunately, most of the temperature soundings made on or after 00 local time indicate that a thick layer (of the order of 500 m) of air from the Gulf of Carpentaria was overspreading the Daly Waters area. Passage of this air mass, frequently having a lapse rate between adiabatic and isothermal, is evident by a temperature increase at the surface, and a decrease over the thick layer aloft. Clearly, such an advective phenomenon violates the assumptions made earlier regarding horizontal uniformity. As a result, only the early evening soundings could be used in this study.

Fig. 2 shows the nocturnal Koorin data plotted in dimensionless coordinates. The exponential curve from Fig. 1 with $a = 0.77$ also turns out to exactly describe the least-squares best fit for the Koorin data. A total of 266 data points are plotted, based on 33 observation times (see Table 2). 96% of the total variance is explained by the exponential curve, over the range $0 < z/H < 9$. 94% of the

Table 1. *Wangara nocturnal length scales (H) and surface temperature decreases ($-\Delta\theta_s$)*

Day/hour	$-\Delta\theta_s$ (K)	H (m)	Day/hour	$-\Delta\theta_s$ (K)	H (m)
1/18	4.4	34	14/06	11.7	96
1/21	7.0	65	19/00	5.9	135
2/00	7.1	101	19/03	8.0	158
6/18	4.2	12	19/06	8.5	183
6/21	7.4	45	30/21	4.0	104
7/03	13.8	62	31/00	5.6	146
7/06	11.9	84	31/03	6.5	185
7/21	9.0	45	31/06	8.0	194
8/00	10.0	63	31/21	6.2	72
11/21	4.2	68	32/00	8.0	90
12/00	6.8	110	32/03	9.3	112
12/06	11.4	119	32/06	11.0	115
12/21	7.2	58	33/00	8.9	85
13/00	9.5	76	33/03	10.3	101
13/03	9.5	108	33/21	8.1	59
13/06	12.8	100	34/00	12.8	61
13/18	5.6	20	34/03	12.5	85
13/21	9.0	40	34/06	12.0	113
14/00	11.3	49	34/18	3.3	34
14/03	12.9	64	34/21	8.5	60

total variance is explained over the subinterval of $0 \leq z/H \leq 5$.

The Koorin data set verify the applicability of the similarity approach, and confirms that the exponential curve (3) adequately describes the structure of these Australian nocturnal temperature inversions.

7. Physical significance of the length scale

The heat-flux-history length scale (2) is strongly modified by the turbulence in the NBL. Given identical values of Q_H during identical time periods, larger length scales correspond to more turbulence.

Table 2. *Koorin nocturnal length scales (H) and surface temperature decreases ($-\Delta\theta_s$)*

Day/hour	$-\Delta\theta_s$ (K)	H (m)	Day/hour	$-\Delta\theta_s$ (K)	H (m)
1/21	12.0	27	16/21	11.3	34
2/21	9.8	30	17/21	10.0	29
3/21	11.0	30	18/21	7.4	32
4/19	4.5	32	19/19	2.9	47
4/21	9.5	34	19/21	6.0	56
5/21	9.3	49	20/00	8.7	77
7/21	7.2	61	20/21	7.9	44
8/20	8.0	38	21/00	10.9	54
9/21	5.8	64	21/21	7.6	43
10/21	6.9	49	23/21	12.9	25
11/21	5.4	73	24/21	11.0	26
12/21	8.5	78	25/21	11.0	34
13/21	9.1	37	26/00	12.6	48
14/19	6.0	30	26/21	10.0	41
14/21	11.2	32	27/21	6.5	58
15/19	5.4	28	29/21	6.8	52
15/21	10.5	31			

Usually, this means a turbulent layer of greater thickness, but the turbulence could additionally be more intense and/or more frequent. The net result of this increased turbulence is to distribute the specified amount of total cooling throughout a thicker layer, leaving a smaller temperature decrease at the surface. By relating H to turbulence in this manner, one is implicitly assuming that turbulence is the dominant mechanism for changing the profile shape.

For example, consider the two potential temperature profiles plotted in Fig. 3. Both of these Koorin soundings were made at 21 local time, and the integrated heat fluxes since transition are within 1% of each other. Yet the surface temperature decrease and the length scales for these two cases are significantly different from each other. Such profile differences may be indicative of the different turbulent histories of each day. Regardless of these differences, both profiles are similar when plotted within the dimensionless framework of Fig. 2.

One might normally expect H to increase with time because of the accumulation nature of that

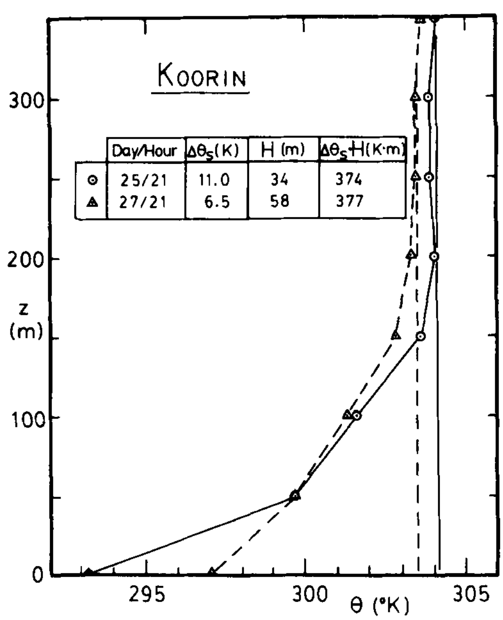

Fig. 3. Sample 21 local-time potential-temperature profiles from the Koorin experiment, showing that the same amount of cooling can be distributed in different ways within the nocturnal boundary layer. The corresponding length and temperature scales are tabulated within the insert.

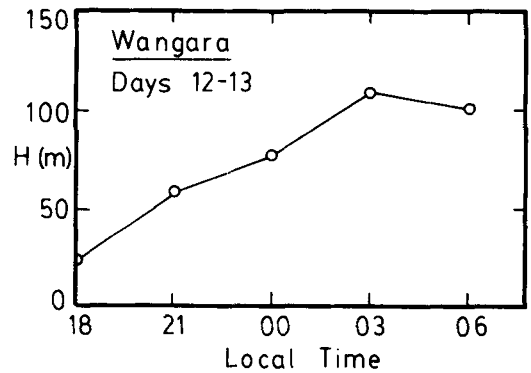

Fig. 4. Change of the heat-flux-history length scale with time during one night, showing that decreases as well as increases of the scale are possible.

scale. However, a pronounced decrease in turbulence may actually cause a decrease in H. Fig. 4 displays a case from the Wangara experiment where the length scale first increases, and then decreases during the course of the night. This suggests a sequence of events where turbulence within a relatively thick layer decays, allowing a thinner layer of cooler temperatures to evolve later in the night.

Another physical interpretation is possible by employing the first law of thermodynamics. Neglecting advection, the statement of conservation of heat can be integrated over time (since transition) and over height (surface to some fixed reference height, z_R, well above the top of the layer of cooled air) to yield

$$\int_0^{z_R} (\theta - \theta_0)\, \mathrm{d}z = \int_0^t (Q_H/\rho C_p)\, \mathrm{d}\tau + R \tag{4}$$

or

$$\int_0^{z_R} \Delta\theta\, \mathrm{d}z = H\, \Delta\theta_s + R \tag{5}$$

where R represents the net direct radiational heating (in the kinematic units of K m) of the whole layer of air between z_R and the surface, during time period t.

If there is no direct radiational cooling of the air, then (5) tells us that the area under the potential temperature profile equals the area enclosed by a rectangle of sides $\Delta\theta_s$ and H. Given the empirical profile described by (3), one discovers that the former area exceeds the latter area (Fig. 5). This tells us that radiational cooling of the air can not be neglected.

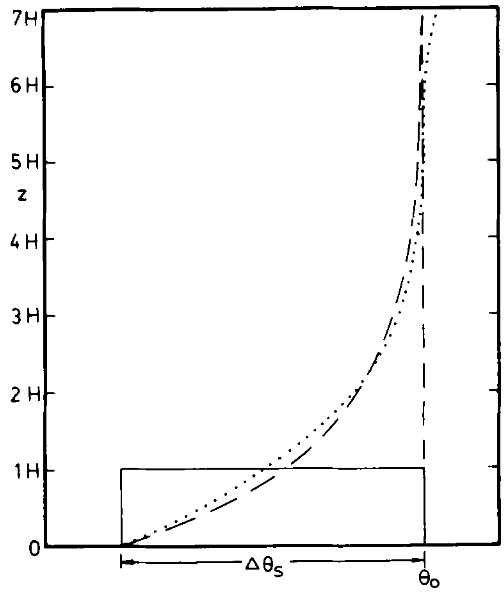

Fig. 5. The relationship between the heat-flux-history length scale and the exponentially-shaped potential temperature profile (dashed line) are sketched. Note that the areas under the solid and dashed lines would be equal if there were no direct radiational cooling of the air. The dotted line shows Yamada's (1979) cubic polynomial, assuming $h = 5H$.

In fact, by integrating (3) over height, one discovers that

$$\int_0^{z_R} \Delta\theta \, dz = H \, \Delta\theta_s / a \tag{6}$$

Given that $a = 0.77$, we find by comparing (5) and (6) that 23% of the total boundary cooling is due to radiation from the air directly, compared to 77% due to turbulent and molecular transport to the ground.

One might expect "a" to be a function of many parameters, such as the relative humidity or the concentration of other constituents within the nocturnal boundary layer. The Wangara and Koorin experiments were both conducted at nearly uninhabited sites that were relatively dry. This could explain why $a = 0.77$ worked so well for both cases. A different value of "a" may be better at other sites.

8. Applications and discussion

Suppose one defines the top of the nocturnal stable layer, h, as that height where the potential temperature decrease is just 2% of that at the surface. Given the exponential shape of the potential temperature profile (3), this top of the inversion occurs at about $h = 5H$. Fig. 6 shows a scatter diagram of the parameterized NBL depth ($h = 5H$) versus the actual depth (h at 2% of the surface temperature decrease) for both the Wangara and Koorin data sets. The corresponding linear correlation coefficient is 0.85.

To use the similarity profile of eq. (3) or Fig. 1, one must know both $\Delta\theta_s$ and H. Knowledge of one of these two, plus knowledge of the heat flux forcing at the surface is sufficient to determine the other variable. For example, easily accessible observations of the early morning surface temperature and estimates of the nocturnal surface heat flux histories are sufficient to use (2) and (3) to estimate the thickness of the nocturnal temperature inversion.

To forecast the depth and temperature decrease within a nocturnal inversion, one must derive a forecast equation for either $\Delta\theta_s$ or H (in addition to forecasting or specifying the surface heat flux). Some methods for forecasting a turbulence-related length scale have been suggested by Mahrt (1981), Nieuwstadt and Tennekes (1981), Smeda (1979), and Deardorff (1971, see Yu, 1978). For example, in Mahrt's (1981) case study based on Wangara day 33–34, forecasts of his nocturnal length scale correspond almost exactly to twice the values of H

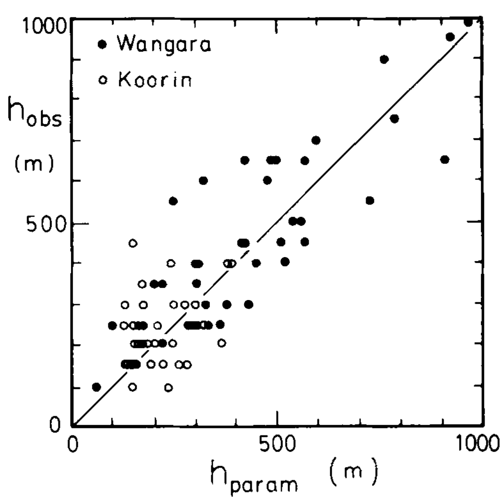

Fig. 6. Parameterized ($h = 5H$) versus observed depths of the nocturnal stable layer for the Wangara (●) and Koorin (O) data sets.

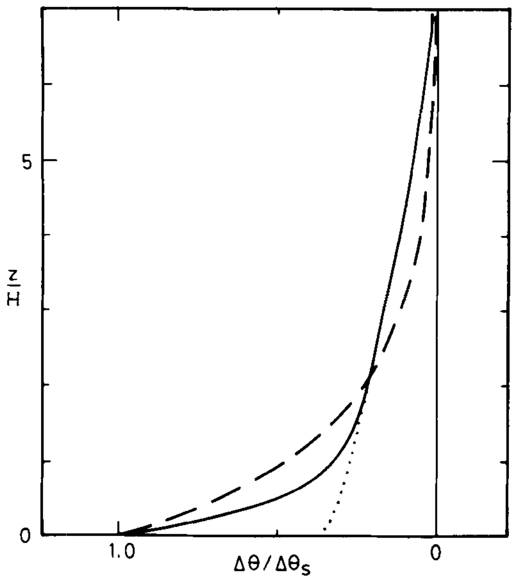

Fig. 7. Sample idealized comparisons of a complex-shaped nocturnal potential temperature profile (solid line) with the corresponding bulk parameterization (dashed line) given by (3). The structure indicated by the solid line might occur when a very windy (turbulent) period is followed by a period of lighter winds.

diagnosed here for the same period. In a companion paper (Stull, 1983), a diagnostic relationship for H is formulated as a function of geostrophic wind speed, wind run, and surface characteristics.

Growth of the stable layer as a function of downwind distance can be described by a generalized form of (2). For steady-state warm-air advection over a colder surface, replace $\mathrm{d}t$ by $\mathrm{d}x/\bar{U}$. Thus:

$$H(X) = \int_0^X (Q_\mathrm{H}(x)/\rho C_p)\ \mathrm{d}x / |\bar{U}(\theta_\mathrm{s}(X) - \theta_\mathrm{s}(0))| \tag{7}$$

where X is the distance downwind from the change in surface temperature. The mean wind speed, U, must be a representative layer-average value.

The exponential profile can provide a simple bulk parameterization scheme for the NBL without resorting to either a slab model or a multi-level model. To illustrate the nature of this bulk parameterization, picture an idealized nocturnal boundary layer where an initial period of more intense turbulence is followed by a period of less intense turbulence. The resulting actual potential temperature profile as illustrated by the solid line in Fig. 7 would be parameterized by the dashed line given by (3). The parameterized curve obviously misses the detailed structure of the sounding, but successfully approximates the bulk strength and depth of the stable layer.

If the Coriolis parameter were an important term in describing the behavior of the nocturnal temperature inversion, then one would expect to see some difference in similarity shapes between the Wangara and the Koorin experiments. Koorin is located at a latitude of 16.3° S, while Wangara is located at 34.5 °S. This means that the Coriolis parameter varies by a factor of two, from 4.1×10^{-5} to $8.3 \times 10^{-5}\ \mathrm{s}^{-1}$, between the two sites. Although the Coriolis parameter may be critical in nocturnal wind calculations, it appears from Figs. 1 and 2 to be not directly important for temperature length-scale calculations. Variables constructed from the Coriolis parameter, such as the Ekman depth, u_*/f, should be used with similar caution.

9. Relationship of H to a rate equation

Nieuwstadt (1980) and Yamada (1979) suggested that the NBL depth adjusts towards an equilibrium height, h_e. To see how such an adjustment equation is related to H, start with (2), the definition of H, and take the time derivative of both sides to give:

$$\Delta\theta_\mathrm{s}\,\mathrm{d}H/\mathrm{d}t + H\,\mathrm{d}\theta_\mathrm{s}/\mathrm{d}t = Q_\mathrm{H}/\rho C_p$$

Solving for $\mathrm{d}H/\mathrm{d}t$ gives

$$\frac{\mathrm{d}H}{\mathrm{d}t} = \frac{(Q_\mathrm{H}/\rho C_p) - H\,\mathrm{d}\theta_\mathrm{s}/\mathrm{d}t}{\Delta\theta_\mathrm{s}} \tag{8}$$

To put this into Nieuwstadt's form, it is necessary to assume that $Q_\mathrm{H} = \rho C_p\,\overline{w'\theta_\mathrm{s}'}$ and $h = bH$, where b is a constant to be defined later. We then find that

$$\mathrm{d}h/\mathrm{d}t = (h_\mathrm{e} - h)/T_\mathrm{D} \tag{9}$$

where

$$T_\mathrm{D} = \Delta\theta_\mathrm{s}/(\mathrm{d}\theta_\mathrm{s}/\mathrm{d}t) \tag{10}$$

and

$$h_\mathrm{e} = b\,\overline{w'\theta_\mathrm{s}'}/(\mathrm{d}\theta_\mathrm{s}/\mathrm{d}t) \tag{11}$$

These three equations are identical to Nieuwstadt's (9), (10), and (7) respectively.

Some comparisons are in order. First, Yamada's assumption regarding radiation had to be neglected by Nieuwstadt to arrive at the above three equations, whereas no assumption regarding radiation was necessary in the derivation given here. Perhaps Yamada's radiation distribution assumption is not appropriate to real boundary layers.

Second, given Yamada's cubic equation for the potential temperature profile, Nieuwstadt's solution gives $b = 4$. If $h = 4H$, then the top of the boundary layer is implicitly defined as that height where the temperature decrease ($\Delta\theta$) is about 5% of the near-surface temperature decrease ($\Delta\theta_s$). Compare this is to the 2% criterion used in section 8, which implied that $h = 5H$. In other words, the role of the physics is being obscured by unnecessary assumptions regarding the profile shape and the 5% versus 2% cut-off definitions of h. This uncertainty can be avoided by using the length scale, H, directly, rather than some arbitrary h.

Finally, (2) is a simple and concise formulation that expresses essentially the same information as the more complicated set of rate equations (9)–(11). Rate equations have been attractive mechanisms for the modeling of NBL's because they allow a time variation of h, and they suggest the existence of an equilibrium depth (even though it may never be reached). Eq. (2) is about as easy to use as a diagnostic expression, and does not depend on assumptions regarding radiation distribution or profile shape. Yet, it is easy to incorporate radiation into a simple profile equation, such as in (3).

10. Summary and conclusion

It is proposed in this paper that the time-integrated value of surface heat flux is more important in describing the nocturnal boundary layer than the instantaneous value of heat flux.

Two scales are defined to be used with nocturnal potential temperature profiles. One, a temperature scale is the surface temperature change since the evening heat flux transition from positive to negative. This scale is defined by $\Delta\theta_s = \theta_s(t) - \theta_0$, where surface temperatures are measured at standard screen height. The other scale is a heat-flux-history length scale, H, defined by (2). This scale employs the time-integrated value of surface heat flux.

Using these scales, one can create a dimensionless height, z/H, and a dimensionless potential temperature, $\Delta\theta/\Delta\theta_s$. Wangara boundary layer data reveal a similarity shape when plotted in this dimensionless framework. The exponential equation (3) with $a = 0.77$ provides the least-squares best fit to the data. This equation might prove useful as an alternative to Yamada's (1979) cubic polynomial.

An independent test (3), using Koorin boundary layer data reveals that $a = 0.77$ also provides the best fit. This value of a suggests that 77% of the cooling within the nocturnal temperature inversion can be accounted for by turbulent and molecular transport of heat to the ground. The remaining 23% may be due to radiational cooling of the air directly. This supports the arguments of Garratt and Brost (1981) and Andre and Mahrt (1982).

The difference in latitude between Hay (Wangara) and Daly Waters (Koorin), Australia corresponds to a change of the Coriolis parameter by a factor of two. The lack of difference between dimensionless potential temperature profiles for Wangara and Koorin suggests that the Coriolis parameter may not be important here. Hence, care must be exercised when applying quantities such as the Ekman layer depth, u_*/f, to the nocturnal temperature inversion.

The heat flux-history length scale can increase or decrease with time, reflecting the recent time-history of this boundary-layer turbulence. A relationship between turbulence and this scale is introduced in a companion paper (Stull, 1983). The nominal top of the NBL (where $\Delta\theta/\Delta\theta_s = 0.02$) occurs at $h = 5H$.

Finally, the heat flux-history length scale is a simple and concise way of expressing much of the same physics that appears in rate or adjustment equations such as Nieuwstadt's (1980). It allows the actual NBL thickness to vary realistically with time, without explicit reference to the concept of a non-attainable equilibrium thickness.

11. Acknowledgements

Debbie Schiess and Eva Singer deserve thanks for their assistance in preparing this manuscript. Steve Naglic, who spent much effort in the initial attempts to apply the concept of an integral length scale to geostrophic drag coefficients, is recognized here. Partial support for this research came from the National Science Foundation under grant ATM-8210685.

12. Appendix

Tables 1 and 2 give the data periods, temperature scales, and heat flux-history length scales for the Wangara and Koorin data used in this study.

Surface temperatures are based on screen-height (instrument shelter) measurements of the air, roughly 1 m above ground. The actual surface "skin" temperature is not used. This screen temperature method was used for both Wangara and Koorin, even though there were 10 m trees at the Koorin site. The published photographs of the Koorin site (Clarke and Brook, 1979) show a sparse distribution of trees. Thus, radiatively cooled air from the leaf surfaces would be mixed down to the instrument shelter by natural forced and free convection processes.

For each of the Wangara and Koorin potential temperature profiles, there is a well-defined adiabatic region (residual layer) above the nocturnal stable layer. Radiosonde temperature sensor errors are apparent by comparing these residual-layer potential temperatures from sounding to sounding during the course of any one night. Superimposed on the expected continuous radiational cooling of the residual layer is a larger instrumental bias, which makes the residual layer potential temperature appear to randomly jump warmer and cooler from sounding to sounding.

To correct for these biases, the residual layer potential temperature is taken as a reference temperature (θ_0). Cooling lower in the boundary layer ($\Delta\theta$ and $\Delta\theta_s$) is calculated relative to this reference. It is important to recognize that this method not only removes the radiosonde error from the sounding, but also removes a bulk radiational cooling from the whole sounding. Thus, the fact that the empirical parameter "a" is less than unity implies that there is more radiational cooling in the lowest 200 m of the NBL than in the residual layer. This appears to differ from Andre and Mahrt's (1982) conclusion.

Length scales are found using expression (2). The heat flux is calculated from a simple surface radiation and ground flux budget: $Q_H = Q^* - Q_G$, where Q^* is the net radiation towards the earth's surface, and Q_G is the net heat flux into the ground at the surface. For both Australian experiments, Q^* and Q_G were usually negative at night, with heating from the warm ground unable to completely compensate the radiational cooling that occurred. For the Koorin data, net radiation from both masts are averaged to yield Q^*, and soil and grass values of ground flux are averaged to give Q_G. The latent heat flux is neglected in this balance because of the usually dry soil conditions and low humidities at Hay and Daly Waters.

Micrometeorological fluxes published for the Wangara experiment represent half-hour averages centered on the hour. To use this data, reported averages are plotted, and a smooth curve is estimated from the plotted points. This curve is then graphically integrated to find the cooling since transition. Such a graphical procedure is necessary to adequately find the transition time, and account for the cooling since that time.

Published Koorin data, however, represent hour averages starting on the indicated hour. This means that cooling up to an indicated hour should be based on values published under the preceding hours. With this time-shift in mind, integrated cooling since transition is found directly by summing the published fluxes and multiplying by the appropriate time periods. Transition for all the Koorin data is estimated to occur at 18 local time.

Tower-made measurements of the temperature profile are not used in this study. Mast values for the Koorin data represent 1 h averages. Unfortunately, the rapidly varying state of the nocturnal boundary layer immediately after transition time makes it impossible to match together the averaged mast and instantaneous radiosonde data. Hence, only the radiosonde data are used.

REFERENCES

Andre, J. C. and Mahrt, L. 1982. The nocturnal surface inversion and influence of clear-air radiative cooling. *J. Atmos. Sci. 39*, 864–878.

Brost, R. A. and Wyngaard, J. C. 1978. A model study of the stably stratified planetary boundary layer. *J. Atmos. Sci. 35*, 1427–1440.

Clarke, R. H. and Brook, R. R. 1979. *The Koorin Expedition, atmospheric boundary layer data over tropical savannah land.* Australian Government Publishing Service, Canberra, Australia. 359 pp.

Clarke, R. H., Dyer, A. J., Brook, R. R., Reid, D. G. and Troup, A. J. 1971. *The Wangara Experiment: Boundary layer data*, CSIRO Austalia, Division of Meteorological Physics, Tech. Paper No. 19.

Deardorff, J. W. 1971. Rate of growth of the nocturnal boundary layer. Paper presented at the Symposium on Air Pollution, Turbulence, and Diffusion, Las Cruces, NM., NCAR ms. No. 71–246.

Garratt, J. R. and Brost, R. A. 1981. Radiative cooling effects within and above the nocturnal boundary layer. *J. Atmos. Sci. 38*, 2730–2746.

Izumi, Y. and Barad, M. L. 1963. Wind and temperature variations during development of a low-level jet. *J. Appl. Meteorol. 2*, 668–673.

Mahrt, L. 1981. Modelling the depth of the stable boundary layer. *Boundary-Layer Meteorol. 21*, 3–19.

Nieuwstadt, F. T. M. 1980. A rate equation for the inversion height in a nocturnal boundary layer. *J. Appl. Meteorol. 19*, 1445–1447.

Nieuwstadt, F. T. M. and Tennekes, H. 1981. A rate equation for the nocturnal boundary layer height. *J. Atmos. Sci. 38*, 1418–1428.

Smeda, M. 1979. Incorporation of planetary boundary-layer processes into numerical forecasting models. *Boundary Layer Meteorol. 16*, 115–129.

Stull, R. B. 1983. Empirical relationships for a nocutrnal length scale. Submitted to the *J. Appl. Meteorol.*

Wetzel, P. J. 1982. Toward parameterization of the stable boundary layer. *J. Appl. Meteorol. 21*, 7–13.

Yamada, T. 1979. Prediction of the nocturnal surface inversion height. *J. Appl. Meteorol. 18*, 526–531.

Yu, T. 1978. Determining the height of the nocturnal boundary layer. *J. Appl. Meteorol. 17*, 28–33.